[10] Brown, C. E., "Aerodynamics of Wake Vortices," *AIAA Journal*, Vol. 11, No. 4, April 1973, pp. 531–536.
[11] Betz, A., "Behavior of Vortex Systems," TM 713, 1933, NACA.
[12] Moore, D. W. and Saffman, P. G., "Axial Flow in Laminar Trailing Vortices," *Proceedings of the Royal Society* (London), Ser. A, Vol. 333, 1973, pp. 491–508.

# Finite-Thickness Diffusion Flames over a Pyrolyzing Fuel Plate

HAROLD KERZNER* AND HERMAN KRIER†
*University of Illinois at Urbana-Champaign, Urbana, Ill.*

### Nomenclature

$B$ = nondimensional heat feedback ratio[3]
$C_p$ = specific heat of a gas species, cal/g°K
$f$ = nondimensional stream function
$f'$ = nondimensional velocity = $u/u_e$
$K_1$ = nondimensional surface blowing parameter[3]
$K_2$ = nondimensional surface activation energy ($K_2 = E_w RT_e$)
$l$ = density-viscosity ratio = $\rho\mu/\rho_e\mu_e$
$\hat{M}$ = molecular weight, g/g-mole
$m, n$ = order of reaction for oxidizer and fuel, respectively
$Q$ = flame heat release, cal/g
$T$ = temperature, °K
$u$ = $x$-component of velocity, cm/sec
$v$ = $y$-component of velocity, cm/sec
$Y$ = mass fraction
$\alpha_{ox}$ = oxygen/fuel ratio at flame sheet
$\alpha_T$ = nondimensional heat release, $Q/C_p T_e$
$\beta$ = pressure gradient parameter[3]
$\zeta_g$ = Damköhler number[2]
$\eta$ = transformed $y$-component
$\theta$ = nondimensional temperature, $T/T_e$
$\mu$ = absolute coefficient of viscosity
$\nu', \nu''$ = stoichiometric coefficients
$\rho$ = density, g/cm³
$\phi$ = fuel/oxygen mass ratio (stoichiometric ratio)

*Subscripts*

$e$ = boundary-layer edge
$( )_\eta$ = differentiation with respect to $\eta$
$( )_s$ = differentiation with respect to $s$
$w$ = wall (fuel surface)
$i$ = species index
$F$ = fuel
$ox$ = oxidizer
$\infty$ = freestream conditions
$+$ = upper side of fuel wall
$-$ = lower side of fuel wall

### Introduction

THE analysis of chemically reacting viscous flows has been greatly simplified by considering the limiting cases of equilibrium and frozen flow. The reader is referred to the classical monographs by Lees[1] and Chung.[2] For equilibrium flow, as the Damköhler number,‡ $\zeta_g$, approaches infinity, the infinitely thin flame sheet is generated defining the streamline where the fuel and oxidizer concentrations are zero and where a heat and mass source exist. For frozen flows, as the Damköhler number approaches zero, a nonreacting flow limit is defined. Thus, for frozen and equilibrium flows, an explicit source term in the energy and species equations is eliminated. For a detailed analysis of the physical phenomena, see Krier and Kerzner.[3]

In the present case, the fuel is assumed to undergo surface pyrolysis with the chemical reactions represented by Arrhenius Kinetics of second order. The effects of the finite thickness of the flame are characterized by a variable gas-phase Damköhler number. These effects are in addition to the "blowing" effect of the gas added to the boundary layer. Although it can be shown that reactive boundary layers with mass addition do not generally admit similar solutions, such an approximate analysis is presented with results that interpret the physico-chemical processes in the boundary layer.

There are generally two studies of interest in the analysis of finite chemical thermodynamics coupled to flow phenomena. First, the relative thickness of the diffusion flame is a complex function of the Damköhler number. Secondly, one attempts to determine the exact limiting numerical values of Damköhler numbers which reflect either frozen or equilibrium flow.

### Governing Equations

The conservation equations that are employed to simulate finite kinetics may be written as

$$(lf_{\eta\eta})_\eta + \beta[(\rho_e/\rho) - f_\eta^2] = 0 \tag{1}$$

$$(lY_{i\eta})_\eta + fY_{i\eta} - \zeta_g \frac{\hat{M}_i}{\hat{M}} (\nu_i' - \nu_i'') e^{-E/RT} \frac{\rho}{\rho_e}^{m+n-1} Y_f^{\,n} Y_{ox}^{\,m} = 0 \tag{2}$$

$$(l\theta_\eta)_\eta + f\theta_\eta + (\zeta_g Q/C_p T_e)(\rho/\rho_e)^{m+n-1} e^{-E/RT} Y_f^{\,n} Y_{ox}^{\,m} = 0 \tag{3}$$

where

$$\rho_e/\rho = T/T_e = \theta \tag{4}$$

is also employed.

Because of the nonapplicability of the flame sheet, the governing equations are now solved as two-point boundary value problems.§

At $\eta = 0$

$$f(\eta) = K_1 \exp[K_2/\theta(\eta)] \quad (K_1, K_2 \text{ are constants});$$
$$f'(\eta) = 0; \qquad f(\eta) = -B\theta'(\eta);$$
$$Y_f'(\eta) + f(\eta)[Y_f(\eta) - Y_{f-}(\eta)] = 0; \quad Y_{ox}(\eta) = 0 \tag{5}$$

At $\eta \to \infty$

$$f'(\eta) = 1; \qquad Y_{ox}(\eta) = Y_{ox_e}; \qquad \theta(\eta) = 1; \qquad Y_f(\eta) = 0 \tag{6}$$

The numerical scheme for the solution to the governing equations is well known and follows the same procedure as discussed by Krier and Kerzner.[3]

In order to solve the energy and species equations by using a superpositioning procedure, the sources terms must be "quasi-linearized" by assuming that they are known functions of the initial conditions in each iteration. Once solutions for the energy and species equations are found, new iterative solutions are based upon old solutions to the conservation equations.

### Results

Figure 1 shows the wall blowing rate vs freestream oxidizer mass fraction for variable Damköhler number. For the case when $\zeta_g = 1$, the flow is frozen, and the wall blowing rate is constant for all values of $Y_{ox_e}$. As the Damköhler number increases, the wall blowing rate approaches the value of the flame sheet model. Results by Liu and Libby[4] show that for $Y_{ox_e} = 0.23$ and $f_w = -0.045$, frozen flow may be represented by a Damköhler number of 2–5, and equilibrium flow by a Damköhler number of approximately 1000. The results by Liu and Libby, however, were not based upon coupled wall boundary conditions, and numerical breakdown is said to occur for $\zeta_g > 1000$.

In the present study it was found that the wall boundary condition, specifically $f_w = -\beta\theta_{\eta w}$, is the controllng factor in

Received January 25, 1974; revision received March 15, 1974.
Index categories: Boundary Layers and Convective Heat Transfer—Laminar; Reactive Flows.

* Research Assistant, Department of Aeronautical and Astronautical Engineering; presently Associate Scientist, Thiokol Chemical Company, Brigham City, Utah. Member AIAA.
† Associate Professor, Department of Aeronautical and Astronautical Engineering. Member AIAA.

‡ The Damköhler number is the ratio of the characteristic diffusion time to the characteristic chemical reaction time.[2]

§ See Ref. 3, for discussion of the boundary layers used in Eqs. (5) and (6).

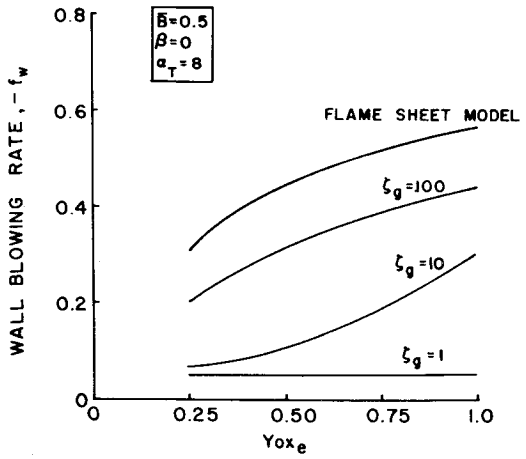


Fig. 1 Wall blowing rate vs freestream oxidizer mass for variable Damköhler number.

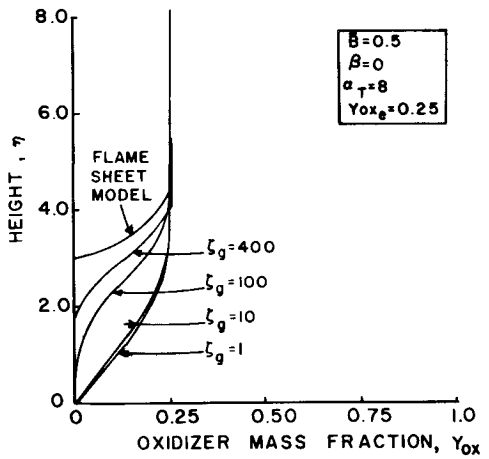


Fig. 3 Height vs oxidizer mass fraction for variable Damköhler number.

determining the maximum Damköhler number before numerical breakdown. For the case when $Y_{ox_e} = 0.25$, the maximum Damköhler number was found to be about 1800. As $Y_{ox_e}$ increases to unity, the maximum Damköhler number is reduced to 1000. The reason for this phenomenon was due to the temperature gradient at the wall. As the wall temperature gradient increases, values of wall blowing rate increase accordingly by the abovementioned wall boundary condition. Although the final value of the wall temperature gradient for the case of finite kinetics is less than for the case of infinite kinetics, the numerical scheme produces large wall temperature gradients such that the magnitude of the wall blowing rate exceeds unity and boundary-layer separation occurs.

This type of numerical degrading is not uncommon in finite kinetics problems. Using matrix techniques for the solution to the conservation equations, Faye and Kaye[5] were apparently the first to identify this problem. Lomax[6] defined this difficulty as due to a "parasitic eigenvalue."

As the Damköhler number increases, convergence from iteration to iteration becomes poor. The source for poor convergence for large Damköhler numbers results in the matrix, which determines the arbitrary constants multiplying the complementary solution, becoming progressively more ill-conditioned.

In Fig. 2, we find that for the values of the Damköhler numbers considered, the fuel mass fraction approaches zero at a streamline of $\eta = 4$. We also notice that the relative change in profiles between $\zeta_g = 100$ and $\zeta_g = 400$, is very small compared to changes between $\zeta = 10$ and $\zeta_g = 100$. The difference between the fuel mass fractions for a Damköhler number of 400 differs by less than 10% from the flame sheet model.

The oxidizer profile is represented in Fig. 3. We find a sharp decrease in wall oxidizer mass fraction between Damköhler numbers of 10 and 100. Unlike the fuel mass fraction profiles, we find that the relative location where the oxidizer profiles approach zero varies between Damköhler numbers. By subtracting the relative flame positions where the fuel and oxidizer profiles are approximately zero, we can determine the relative thickness of the flame zone. If we define the flame zone "thickness" as the region where both the fuel and oxidizer exist in measurable amounts (say $Y_{ox} \simeq 0.05 Y_{ox_e}$; $Y_f = 0.05 Y_{f_w}$), then Figs. 2 and 3 indicate tht the flame zone thickness is proportional to $\zeta_g^{-1/5}$.

The key observations were the following.

a) The fuel regression (blowing) rate approaches a maximum value for the infinite kinetic gas-phase rates, and that Damköhler numbers of the order of 100 provide for such a maximum $f_w$. Numerically solutions of $\zeta_g > 1000$ are possible but provide little information not already available at lower numbers.

b) The combustion "zone" at these intermediate Damköhler numbers $[\zeta_g = 0(100)]$ was significant compared to the boundary-layer thickness. This means that an experimentally observed finite combustion zone (in laminar flow) would not necessarily imply that the regression rate is *not* the maximum.

c) Flame sheet analyses always predict upper limits of flame temperature and species mass fraction, but generally provide a good representation of convective chemically reactive flows.

d) The flame zone thickness is a function of the Damköhler number as required, but this thickness is approximately proportional to $\zeta_g^{-1/5}$, a weaker function than the theoretical relation $\zeta_g^{-1}$ as discussed by Krishnamurthy and Williams.[7]

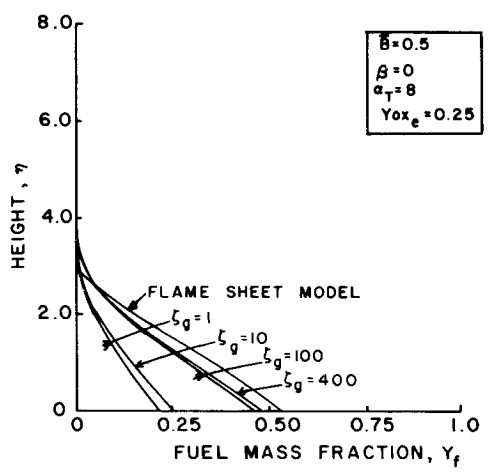


Fig. 2 Height vs fuel mass fraction for variable Damköhler number.

## References

[1] Lees, L., "Convective Heat Transfer with Mass Addition and Chemical Reactions," *Combustion and Propulsion: Third AGARD Colloquium*, Pergamon Press, New York, 1958, pp. 451–497.

[2] Chung, P. M., "Chemically Reacting Non-Equilibrium Boundary Layers," *Advances in Heat Transfer*, Vol. 2, Academic Press, London, 1965, pp. 110–268.

[3] Krier, H. and Kerzner, H., "An Analysis of the Chemically Reacting Laminar Boundary Layer During Hybrid Combustion," *AIAA Journal*, Vol. 11, No. 12, Dec. 1973, pp. 1691–1698.

[4] Liu, T. M. and Libby, P. A., "Boundary Layer at Stagnation Point with Hydrogen Injection," *Combustion and Science Technology*, Vol. 2, 1970, p. 131.

[5] Faye, J. A. and Kaye, H., "A Finite-Difference Solution of Similar Nonequilibrium Boundary Layers," *AIAA Journal*, Vol. 5, No. 11, Nov. 1967, pp. 1949–1954.

[6] Lomax, H., "An Operational Unification of Finite Difference Methods for the Numerical Integration of Ordinary Differential Equations," TR-R-262, 1967, NASA.

[7] Krishnamurthy, L. and Williams, F. A., "Kinetics and Regression," *SIAM Journal of Applied Mathematics*, Vol. 20, 1971, pp. 590–611.

# Supersonic Laminar Base Pressure, Heat-Transfer, and Upstream Influence Correlations for Small Steps

G. R. INGER*
*Virginia Polytechnic Institute and State University, Blacksburg, Va.*

## Introduction

MOST studies of supersonic boundary-layer flow past a rearward-facing step have dealt primarily with the Chapman-Korst limit where the step height $h$ is large compared to the incoming boundary-layer thickness $\delta$ and the resulting expansion around the corner is essentially a rotational inviscid flow problem. Far less has been done for high Reynolds number flows in the opposite limit of a small step such that $h/\delta \ll 1$. However, this latter situation is of considerable practical interest; for example, in connection with structural skin joint faults on large high-speed vehicles such as the Space Shuttle where the heat-transfer and pressure disturbances around such small steps or gaps is of concern.

This Note describes some results of the application of a unified theory of small disturbances in nonuniform high-speed boundary layers[1] to this small-step problem for the case of supersonic laminar nonadiabatic flow. Comparisons with experimental data will be given which show good agreement in a variety of physical features, including useful new base pressure and heat-transfer correlation relations.

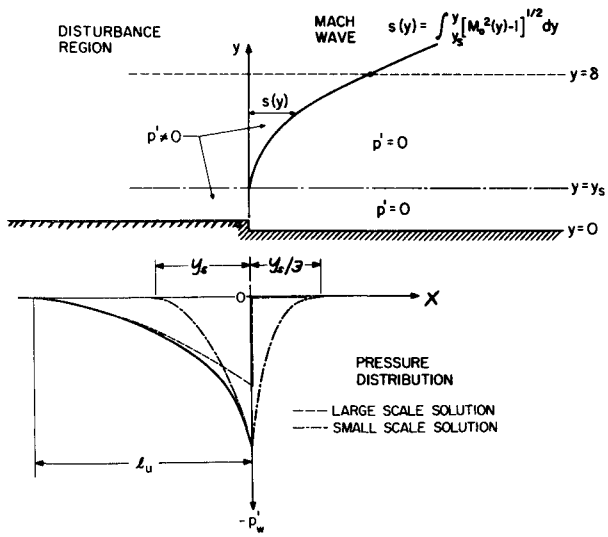


**Fig. 1 Large scale features of pressure disturbance field (schematic).**

Received January 31, 1974. This work was supported by NASA under Contract NAS 1-10646-4.

Index category: Boundary Layers and Convective Heat Transfer—Laminar.

* Professor of Aerospace and Ocean Engineering. Associate Fellow AIAA.

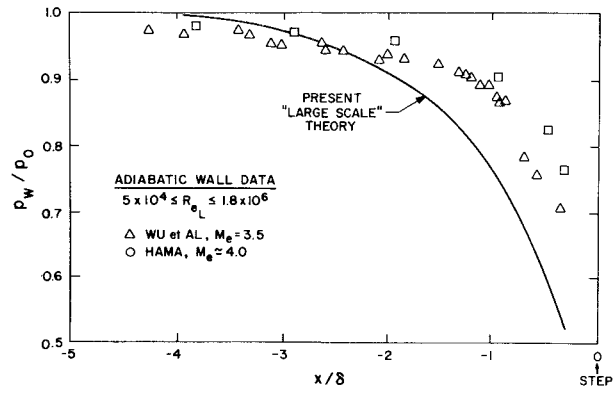


**Fig. 2 Wall pressure distribution upstream of step.**

## Theory and Experiment

Using a small perturbation approach, an analytical theory was developed that predicts the steady-state pressure, temperature, and heat-transfer disturbance fields including suction or blowing through the step.[2] Particular emphasis was placed on the important effects of the highly nonuniform flow across the boundary layer, lateral pressure gradients, and the upstream influence associated with viscous-inviscid interaction. Approximate analytical expressions for the wall pressure, skin-friction, and heat-transfer perturbations and upstream influence distance were derived by a Fourier transformation approach.

The leading approximation for the large-scale pressure disturbance field along the wall is found[2] to vanish downstream of the step $x > 0$ (Fig. 1), while upstream behaving like

$$p_w'/\gamma P_o \approx (-h/l_u)[M_o^2(y^*)/(M_{o_e}^2 - 1)^{1/2}]e^{x/l_u} \qquad (1)$$

where $M_o(y^*)$ is the boundary-layer profile Mach number at the edge $y = y^*$ of the Lighthill viscous disturbance sublayer and $l_u$ is the upstream distance given by

$$u_e l_u/\nu_e \approx 2.9(T_w/T_e)^{5/4}(Cf_o)^{-5/4}(M_{e_o}^2 - 1)^{-3/8}$$

with

$$y^*/l_u \approx 0.49 C_{f_o}^{1/2}(M_{e_o}^2 - 1)^{1/4}$$

and $C_{f_o}$ is the undisturbed flow skin-friction coefficient. A comparison of this prediction for laminar flow with some experimental upstream wall pressure distributions[3] is shown in Fig. 2. The boundary-layer anticipation of the corner expansion is seen to be reasonably well described by the present linearized theory with an over-all upstream influence distance that is relatively insensitive to the step height.

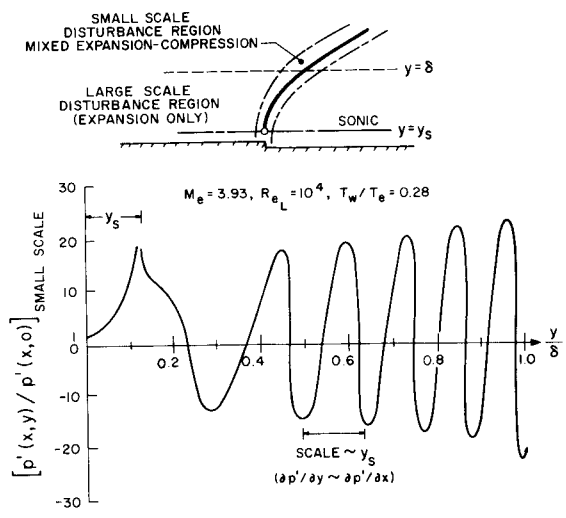


**Fig. 3 Small-scale perturbation structure.**